XA0400444

IC/IR/2004/2
INTERNAL REPORT
(Limited Distribution)

40th anniversary 1964 2004

United Nations Educational Scientific and Cultural Organization
and
International Atomic Energy Agency
THE ABDUS SALAM INTERNATIONAL CENTRE FOR THEORETICAL PHYSICS

DENSITY DEPENDENCE OF THE DIFFUSION COEFFICIENT OF ALKALI METALS

G.A. Adebayo[1]
Department of Physics, University of Agriculture, Abeokuta, Nigeria
and
The Abdus Salam International Centre for Theoretical Physics, Trieste, Italy,

B.C. Anusionwu[2]
Department of Physics, Federal University of Technology, Owerri, Nigeria
and
The Abdus Salam International Centre for Theoretical Physics, Trieste, Italy

and

A.N. Njah, B. Mathew and O.A.T. Fabamise
Department of Physics, University of Agriculture, Abeokuta, Nigeria.

MIRAMARE – TRIESTE

June 2004

[1] Junior Associate of the Abdus Salam ICTP. E-mail: gadebayo@ictp.trieste.it
[2] Junior Associate of the Abdus Salam ICTP.

Abstract

The effect of density on transport coefficients of liquid Li, Na and K at high temperatures using the method of Molecular Dynamics simulation has been studied. Simulation of these liquid alkali metals were carried out with 800 particles in simulation boxes with periodic boundary conditions imposed. In order to test the reliability of the interatomic potential used in the calculations, experimental data on the structural properties were compared with calculated results. The calculations showed a linear relationship between the density and the diffusion coefficient in all the systems investigated except in lithium, where, due to the small size of the atom, standard molecular dynamics simulation method may not be appropriate for calculating the properties of interest.

1 Introduction

Alkali metals are being used in electrolyte salts for batteries, however, little has been reported about the diffusion processes in alkali cells. The use of alkali metals in batteries has been around for a long time. Alkali-based batteries are known to be durable and possess long lasting energies. The chemical reactions responsible for the durability of alkali batteries are partly due to the transport properties and the concentrations of the constituent elements. Therefore, a study of the relationship between the diffusion coefficient and the concentration in the alkali metals will provide more insight into how chemical reactions can improve the development of better alkali-based batteries.

The transport properties of simple liquids have been extensively investigated over the years. Theoretical and experimental results abound in literature dealing with thermodynamics, structural and transport properties of simple homogeneous liquid metals [1-3]. In recent years, Wax and coworkers have carried out studies and investigations on the diffusion coefficient of liquid alkali metals [4-6], however, many of these studies are on the temperature dependence of the transport coefficient. Many other studies on alkali metals are focused on temperature dependence of the diffusion coefficient at constant volume line and liquid-gas coexistence curve.

In his work, Tanaka was able to discover that the Arrhenius law is unable to fit the relationship that exists between the diffusion coefficient and temperature in Rb[7]. Other groups have used the Ashcroft pseudopotential and also ab initio MD to study liquid Na, Cs and Rb[8-11].

In this work, we apply the method of molecular dynamics in the microcanonical ensemble to simulate the behaviour of liquid alkali metals' transport cofficient over a range of densities in order to find the relationship that exists between the density and the transport coefficient. We present an extensive study of the diffusion coefficient over some densities range for temperatures close to the melting and above the melting points.

This paper is organized in the following way, in Section 2 we present the computational details alongside the potential model used in our simulation. In section 3, we present the results and discussion while the conclusions are given in Section 4.

2 Formalism and Methodology

The formalism of interatomic pair potential in condensed matter has been presented in a number of literatures [12-15]. However, for reasons of coherence, we present here some of the approaches to a certain extent.

It is possible to write the total energy of a classical system consisting of N pairwise interacting atoms enclosed in a volume V as:

$$v(r_{ij}) = \frac{1}{2}\sum_{ij}\phi(r_{ij}) \tag{1}$$

where $\phi(r_{ij})$ is the pair potential between pair of atoms. The summation in eqn.(1) is a double summation over all atoms, the factor of 2 in the denominator is included to avoid over counting in the summation. The above equation also depends only on the nuclear charges and the interaction distance. We have made the above statement, bearing in mind that our assumption is reasonably well justified only at high energies and may not be as good at low energies. Attractive forces become significant if potentials are required at very low energies. There are a number of commonly used attractive potentials in simulation, because of the simplicity and cost effectiveness. The Morse potential [16] :

$$\phi(r) = D\exp\left[-2a(r-r_o)\right] - 2D\exp\left[-a(r-r_o)\right] \tag{2}$$

can be used to determine the allowed energy levels in molecules. In eqn.(2), the first term represents the repulsive part, while the attractive part, which dominates at large distances, is represented by the second term. The depth of the attractiveness is given by D and r_o is the internuclear distance at which the potential has its minimum. The parameter $'a'$ determines the distance and slope at which the potential reaches zero.

A second type of attractive potential is the Lennard-Jones potential [17], which is used in this work. This potential was initially used for closed shell elements [18 – 20], however, with good choice of parametrization, it is equally good for modelling some other types of systems [21 – 24]. Generally, the Lennard-Jones potential is of the form:

$$\phi(r) = 4\epsilon\left[(\frac{\sigma}{r})^{12} - (\frac{\sigma}{r})^{6}\right] \tag{3}$$

The repulsive term is given by the first term, where the second term, which is induced by the dipole-dipole interactions leading to the weak van der Waals forces, is the attractive part. In eqn.(3), ϵ and σ respectively represent the well depth of the potential and the atomic diameter. The potential is truncated and shifted, this makes the potential and forces not to vanish at distances above the cut-off radius, that is:

$$\phi(r) = \begin{cases} \phi(r_{ij}) - \phi(r_c) & if \quad r \leq r_c \\ 0 & if \quad r > r_c \end{cases} \tag{4}$$

Molecular dynamics simulation (in each run) were performed on a system containing 800 atoms, the simulation box was repeated in space, initial configuration of scc was assigned to atoms in the system, while velocities of atoms were set to zero. The mass, m of an atom is set to unity for convenience. Interactions beyond distance $r_c = \frac{1}{2}L$ are set to zero. In this case L

is the length of the simulation box. The following units were used, distance in unit of σ, energy in unit of ϵ, temperature in unit of $\frac{\epsilon}{K_B}$ and time in unit of $\sigma\sqrt{\frac{m}{\epsilon}}$. The density is given in unit of $\rho\sigma^3$. The initial scc configurations were melted by allowing the Newton's equation of motion to heat up the system from the zero velocity configurations and scaling the velocities with the square root of the ratio of the temperature and the motion energy. The Verlet algorithm was used in the integration of the equation of motion with a time step of $\Delta t = 0.004$, where the total number of time steps is above 3000. This time step is acceptable as long as the energy and momentum are conserved to desired accuracy and that the time step should always be much "shorter" than any relaxation time observed or expected in the system.

The internal energy per atom is calculated as the sum of the potential and kinetic terms, this is given as:

$$E_{Tot} = \frac{1}{N}\left\langle \frac{1}{2}\sum_{i}^{N} m_i v_i^2 + V(r_{ij}) \right\rangle \tag{5}$$

Here, $V(r_{ij})$ is as given in eqn.(1). To calculate the pressure, we use:

$$P = \rho^2\left\langle \sum_{i}^{N} m_i v_i^2 + \sum_{i}^{N-1}\sum_{j>i}^{N} r_{ij}\frac{dV(r_{ij})}{dr_{ij}} \right\rangle \tag{6}$$

To check the accuracy of eqns.(5) and (6), we have calculated same from the pair distribution function $g(r)$ respectively from:

$$\frac{U}{N} = \frac{1}{2}\rho\int_0^\infty g(r)\phi(r)dr \tag{7}$$

$$= 2\pi\rho\int_0^\infty r^2 g(r)\phi(r)dr \tag{8}$$

and

$$P = \rho T - \frac{1}{6}\rho^2\int_0^\infty r^2 g(r)\frac{d\phi(r)}{dr}dr \tag{9}$$

$$= \rho T - \frac{2}{3}\pi\rho^2\int_0^\infty r^3 g(r)\frac{d\phi(r)}{dr}dr \tag{10}$$

Here, $\frac{U}{N}$ is the potential energy per atom.

The pair distribution function has been calculated using:

$$g(r) = \frac{n(r)}{\Delta r\rho} \tag{11}$$

where $n(r)$ is the average number of atoms that can be found between the distance

$$r - \frac{\Delta r}{2} < r < r + \frac{\Delta r}{2} \tag{12}$$

centred around an arbitrary atom. Structural calculations of the $g(r)$ were obtained by collecting configurations during the run at every 5 time steps. We have obtained the $g(r)$ by reading the collected configurations and using the calculated distance between atomic pairs to construct a histogram. Normalization of the histogram was based on the method described in literature [14].

Using the Green-Kubo (GK) relation [25], we calculated the transport coefficients such as the diffusion coefficient D and the viscosity η, we then employed the Einstein relation [25] to recheck the calculated properties. The diffusion coefficient can be calculated by starting with the Fick's law of diffusion

$$j = -D\nabla c \tag{13}$$

where j is the flux of diffusing species, c is the concentration and D is known as the proportionality constant called the diffusion coefficient. The time evolution of the concentration profile of eqn.(13) is then given as [25]

$$\nabla.j(r,t) = -\frac{\partial c}{\partial t} \tag{14}$$

By combination, eqns.(13) and (14) become:

$$\frac{\partial^2 c}{\partial t^2} - D\nabla^2 c = 0 \tag{15}$$

The above equation where $c = c(r,t)$ can be solved with the boundary condition such that:

$$c(r,t) = \delta(r) \tag{16}$$

here, $\delta(r)$ is the Dirac delta function. The solution of eqn.(15) is:

$$c(r,t) = \frac{1}{(2\pi Dt)^{\frac{d}{2}}} \exp\left(-\frac{r^2}{2Dt}\right) \tag{17}$$

where d is the dimension of the system. By imposing the condition that:

$$\int c(r,t)dr = 1 \tag{18}$$

Then the second moment of eqn.(17) will be given as:

$$< r^2(t) >= \int c(r,t)r^2 dr \tag{19}$$

The time evolution of $< r^2(t) >$ is then obtained using eqn.(15):

$$\frac{\partial}{\partial t}\int c(r,t)r^2 dr = D\int \nabla^2 c(r,t)r^2 dr \tag{20}$$

leading to:

$$\frac{\partial < r^2(t) >}{\partial t} = 2dD \tag{21}$$

eqn.(20) is the so-called the Einstein relation, it connects the means square displacement with the diffusion coefficient in liquid systems. The form of eqn.(20) that entered into our simulation is actually:

$$< \Delta r(t)^2 >= \frac{1}{N}\sum_{i=1}^{N} \Delta r_i(t)^2 \tag{22}$$

where $< \Delta r(t)^2 >$ is called the mean square displacement. On the other hand, the Green-Kubo relation for the diffusion coefficient is given as [25] :

$$2D = \lim_{t\to\infty} 2\int_0^t < v(t-t').v(0) > dt' \tag{23}$$

therefore,

$$D = \int_0^\infty < v(\tau).v(0) > d\tau \tag{24}$$

this is the Green-Kubo equation for the diffusion coefficient, where $\tau = t - t'$ and $< v(\tau).v(0) >$ is a measure of correlation between the velocity of an atom at times $t - t'$ and $t = 0$. It is also known as the velocity autocorrelation function.

Similarly, for the viscosity, the Green-Kubo relation is given as [11,22]:

$$\eta = \frac{1}{VK_BT} \int_0^\infty \Big\langle \sigma_{xy}(t).\sigma_{xy}(0) \Big\rangle dt \tag{25}$$

where σ_{xy} is defined as:

$$\sigma_{xy} = \sum_{i=1}^{N} m_i v_{ix} v_{iy} + \frac{1}{2} \sum_{i=1}^{N-1} \sum_{j>i}^{N} r_{ij} f(r_{ij}) \tag{26}$$

All simulations are performed in the microcanonical ensemble, we waited for the total number of time steps of over 1000 for the system to melt from initial configuration and another 2000 time steps before samples were taken for analysis. The time step Δt used in each simulation is such that it is "shorter" than the relaxation time of the system as mentioned earlier on.

3 Results and discussion

We have performed molecular dynamics simulation for liquid alkali metals at different thermodynamic states for which diffraction data are available [26]. In Table 1, we provide the details of the parameters of the Lennard-Jones potential used in our calculation. In all of the simulation runs, single-particle properties of the alkali metals were evaluated to investigate the density dependence of the properties. Tables 2-4 show the summaries of the properties investigated at various reduced densities. All calculations are performed at experimental densities [26].

To investigate the reliabilty of the pair potential used in this calculation, a comparison of the calculated pair distribution function with experiment are presented in Figure 1. We have agreements between experiments and calculations except for the difference in the height of the first peak. In most cases, this can be ascribed to the potential minimum of the modelled pair interactions. From the figure, the peaks of the graph obtained from the simulation is higher than that of the experimental values in liquid Na. The solid lines represent our calculated result while the points represent the experimental result. We can say that at low density and high temperature, there is not much difference between the calculated and experimental structural arrangement of atoms in both liquid Na and liquid K except that there is a slight difference in their first peaks. The agreements with experimental results justify our confidence in the type of pair potential used in this work.

We want to mention here that it was possible to do calculations at only two densities for Li, (Table 2). This is as a result of limited experimental information for liquid Li. The available experimental information used for the two densities given were obtained from Waseda [26]. With these two sets of data points, it is not very clear the kind of curve that exists between the density and diffusion coefficient in liquid Li. We also observed from Figure 1, that at low density and high temperature there is not much difference in the structure or arrangement of atoms in liquid Li. This implies that the structure of liquid Li does not change much within the investigated range.

From Tables 3 and 4, it can be noticed that as density increases the pressure decreases and the total energy increases. In Table 2, the values of pressure obtained for Li are negative. This is in contrast to all other systems investigated. As a result of this, it can be suggested that the method of calculation may not be suitable for calculating the equation of state for lithium. But we note that the same calculation method was used for both liquid Na and K. However, to confirm this, we estimated the de-Broglie thermal wavelength λ and compared it with the lattice parameter $'a'$ of crystalline Li. The result showed that the condition $\frac{\lambda}{a} \ll 1$ is not satisfied. This estimate shows that the standard classical method of Molecular Dynamics simulation is not suitable for systems such as Li, because of its small size. We can only mention here that from Tables 3 and 4, along with Figures 2a and 2b, it can be seen that the diffusion coefficient increases linearly with density.

In Figures 2a and 2b the graphs of the dependence of diffusion coefficient on density for K and Na appear to be not perfectly linear. But it can easily be noticed that the calculated points appear to scatter about a mean line. This non perfect linearity could be attributed to the temperature dependence of the atomic densities. In addition, from Tables 3 and 4, it can be seen that for Na and K liquid metals, as the density decreases with increasing temperature, the pressure decreases and the total energy decreases. In all the systems studied, the negative values of the total energy imply stability in the system at the investigated conditions.

A perusal of Figure 3 shows the oscillations usually found in the small time steps region of the velocity autocorrelation function. These initial oscillations have negative values, but tend to zero at higher temperatures. As density decreases, there is a Gaussian decay of the velocity autocorrelation function causing a reference atom to undergo a motion similar to Brownian in the fluctuating force field of its nearest neighbours.

4 Concluding remarks

The density dependence of the diffusion coefficient of systems (i.e. Li, Na and K) modeled via the Lennard-Jones potential has been investigated. From the results and discussion, it was seen

that the diffusion coefficient of the various liquid alkali metals increases linearly with density. As temperature increases in liquid Na and K, density decreases because atoms are energized to move apart and are spaced out. Although we observed a slight tendency similar to the Arrhenius law for density, in Lennard-Jones 3D alkali liquids, the linear relationship between the density and the diffusion coefficient is more pronounced.

Acknowledgments. This work was done within the framework of the Associateship Scheme of the Abdus Salam International Centre for Theoretical Physics, Trieste, Italy. Financial support from Swedish International Development Cooperation Agency is acknowledged. GAA acknowledges the DAAD for computer equipment grant.

References

[1] S. K. Sharma and K. Tankeshwar, *J. Phys. Condens. Matt.* **8**, *10 839 (1996).*

[2] M. Gerl and A. Gruson, *Handbook of Thermodynamic and Transport Properties of Alkali Metals, ed. R. X. Ohse, Blackwell, Oxf. (1985).*

[3] I. Yokoyama, *Physica B,* **243**, *338 (2001).*

[4] R. Albaki, J. F. Wax and J. L. Bretonnet, *J. Non-crys. Solids,* **312**, *153 (2002)*

[5] J. F. Wax, R. Albaki and J. L. Bretonnet, *J. Non-crys. Solids,* **312**, *187 (2002)*

[6] J. F. Wax, R. Albaki and J. L. Bretonnet, *Phys. Rev. B* **65**, *Art. No.014301 Jan. (2002)*

[7] M. Tanaka, *J. Phys. f. Matt. Phys.* **10**, *10 2581 (1980).*

[8] U. Balucacci, G. Nowomy and G. Kahl, *J. Phys. Condens. Matt.* **9**, *3371 (1971).*

[9] G. Kahl and S. Kambayashi, *J. Phys. Condens. Matt.* **6**, *10897 (1994).*

[10] G. Kahl, *J. Phys. Condens. Matt.* **6**, *10923 (1994).*

[11] S. Gomez, L. E. Gonzalez, D. J. Gonzalez, M. J. Stott, S. Dalgio and M. Silbert, *J. Non-crystalline Solids,* **163**, *250 (1999).*

[12] M. Finnis, *Interatomic Forces in Condensed Matter, Oxf. Univ. Press (2003).*

[13] A. Hinchliffe, *Chemical Modelling: From Atoms to Liquids, John Wiley & Sons (1999).*

[14] J. P. Hansen and I. R. McDonald, *Theory of Simple liquids, Acad. Press Lond. (1986).*

[15] G. Ciccotti and W. G. Hoover, *Ed. Simulazione di sistemi statistico-meccanici con la dinamica molecolare, North-Holland Amsterdam (1986).*

[16] P. M. Morse, *Phys. Rev.* **34**, *57 (1929).*

[17] J. E. Lennard-Jones, *Proc. R. Soc. Lond.*, **A106**, *441 (1924).*

[18] A. Rahman, *Phys. Rev.* **136**, *A405 (1964)*

[19] L. Verlet, *Phys. Rev.* **159**, *98 (1968)*

[20] G. Ciccotti, D. Frenkel and I. R. McDonald, *Simulation of liquids and Solids: Molecular Dynamics and Monte Carlo Methods in Statistical Mechanics, NH Amsterdam (1987)*

[21] W. Kob, C. Donati, S. J. Plimpton, P. H. Poole and Glotzer, *Phys. Rev. Lett.* **79**, *2827 (1997).*

[22] M. P. Moody and P. Attard, *J. Chem. Phys.* **115**, *8967 (2001).*

[23] Y. Qin and K. A. Fichthorn, *J. Chem. Phys.* **119**, *9745 (2003).*

[24] R. M. Yulmetyev, A. V. Mokslun and P. Hänggi, *Phys. Rev. E* **68**, *051210 (2003).*

[25] D. Frenkel and B. Smit, *Understanding Molecular Simulation, From Algorithm to Applications, Acad.Press, London (1986)*

[26] Y. Waseda, *The Structure of non-crystalline materials: liquids and amorphous solids, McGraw-Hill, NY (1980)*

Table 1: The parameters of the Lennard-Jones potential

Element	$\epsilon(K)$	$\sigma(\mathring{A})$
Li	2383.57	2.839
Na	1600.26	3.475
K	1327.55	4.285

Table 2: Thermodynamics properties of liquid Li

T^*	ρ^*	D	Pressure	Total Energy
0.190	0.714	0.04495	-0.633	-5.576
0.194	0.725	0.05237	-0.818	-5.492

Table 3: Thermodynamic properties of liquid Sodium calculated from our simulation

T^*	ρ^*	D	Pressure	Total Energy
0.264	1.016	0.24661	35.212	-1.706
0.295	0.995	0.22503	30.044	-2.319
0.358	0.961	0.21062	22.898	-3.148
0.452	0.932	0.18759	17.828	-3.704
0.576	0.906	0.17540	14.246	-4.070

Table 4: Thermodynamic properties of liquid Potassium calculated from our simulation

T^*	ρ^*	D	Pressure	Total Energy
0.258	1.007	0.22907	33.007	-1.973
0.285	0.991	0.21805	29.251	-2.414
0.356	0.968	0.20754	24.291	-2.985
0.469	0.928	0.19284	17.323	-3.760
0.544	0.897	0.17581	12.800	-4.228

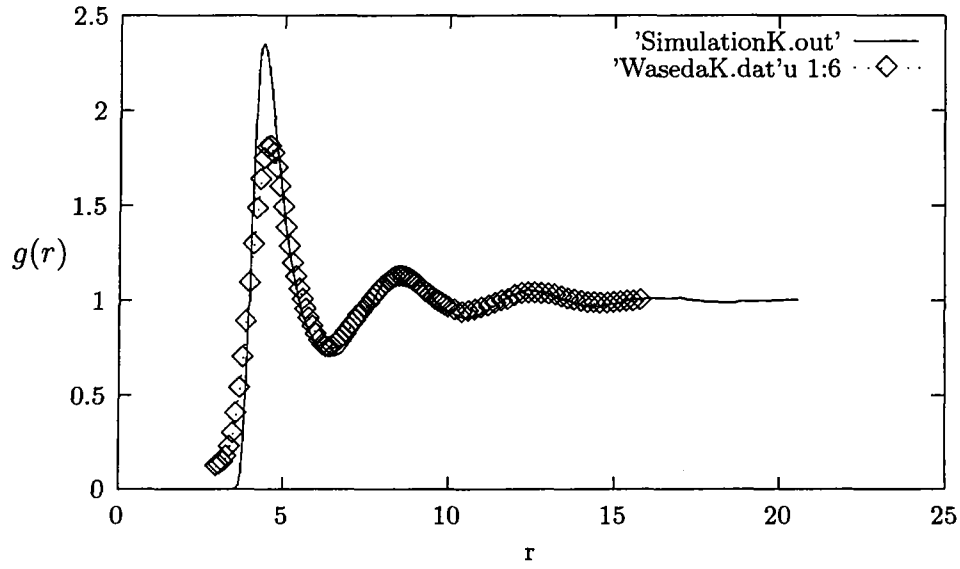

Low density effects on the structure of liquid Na at high temperature

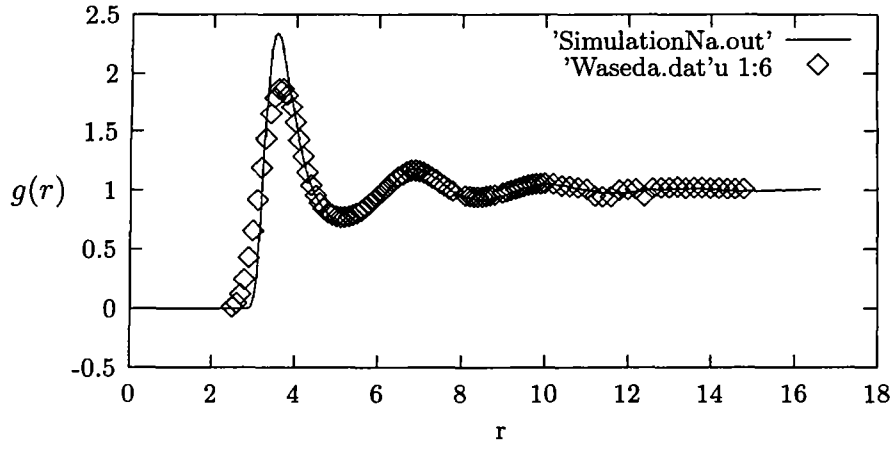

Structural arrangement of atoms in liquid Li at high temperature

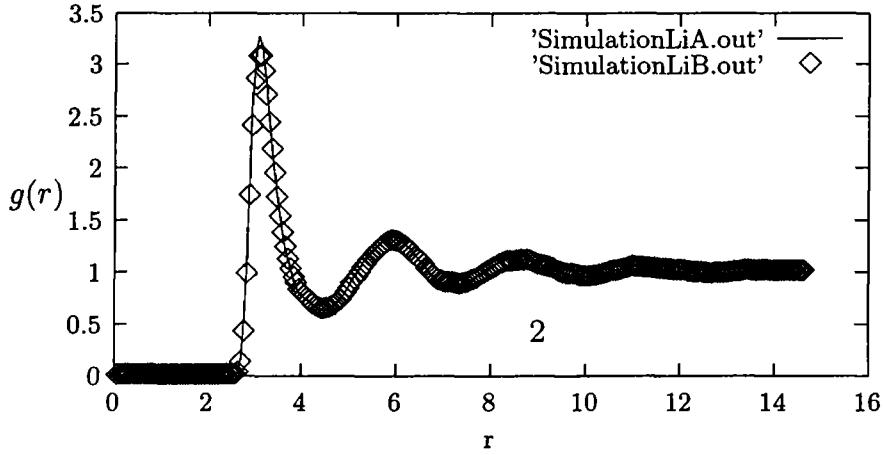

Figure 1: The comparison of calculated results with experiments[24]

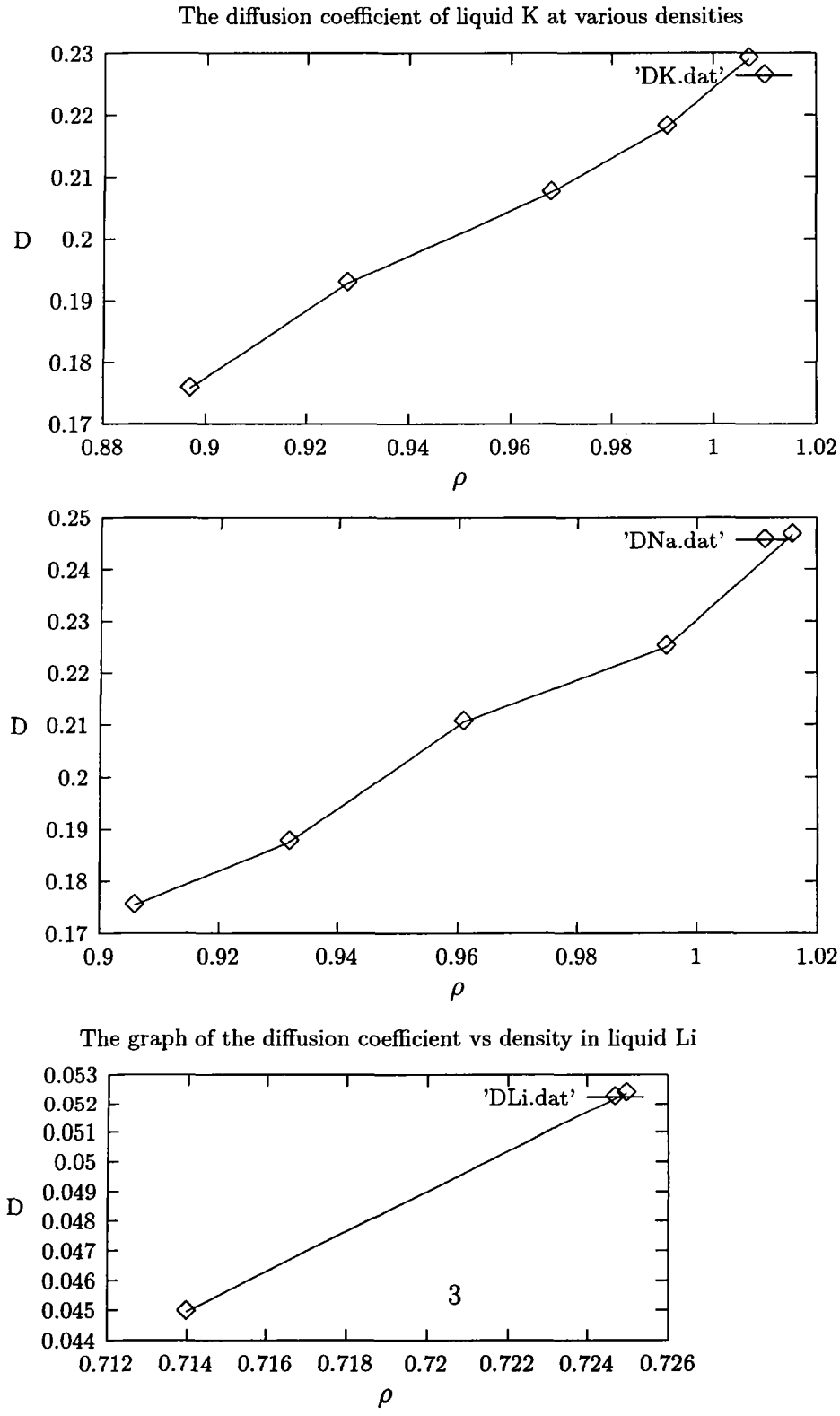

Figure 2: The graph of the Diffusion coefficient in liquid Na at various densities

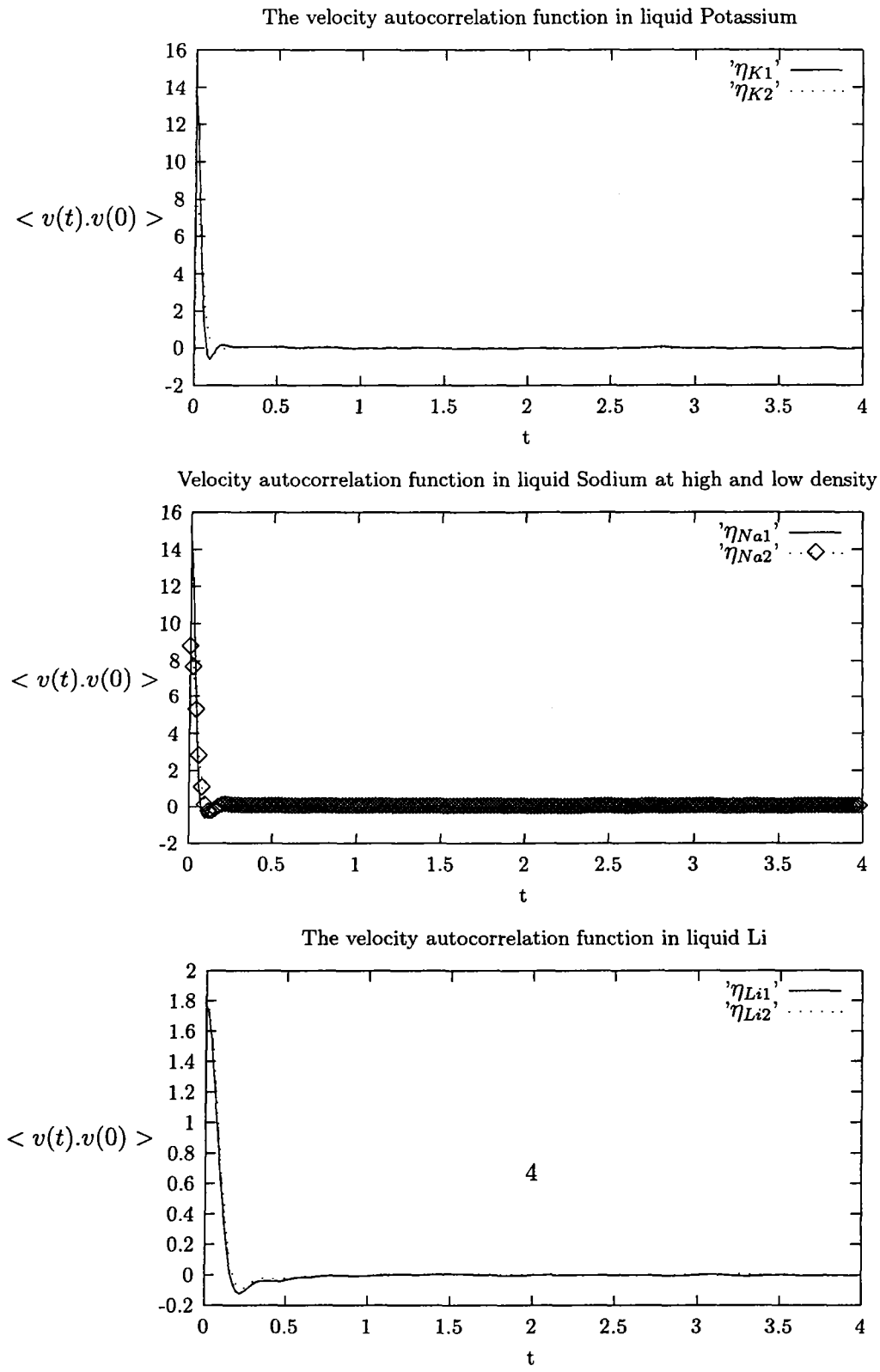

Figure 3: The plot of the velcocity autocorrelation function in liquid Sodium, at low and high densities